Symmetry effects on the optical coupling between plasmonic nanoparticles with applications to hierarchical structures

D. E. Gómez, K. C. Vernon, and T. J. Davis
CSIRO Materials Science and Engineering, Private Bag 33, Clayton, Victoria 3168, Australia
and CSIRO Future Manufacturing Flagship, Gate 5 Normanby Road, Clayton, Victoria 3168, Australia
(Received 7 October 2009; revised manuscript received 10 December 2009; published 16 February 2010)

We present theoretical studies on the collective optical response of symmetric configurations of metallic nanoparticles. We show that within the electrostatic approximation, the surface plasmon resonance of these symmetric multiparticle systems can be expressed as symmetry-adapted linear combinations of the plasmon modes of each particle of the ensemble, closely resembling the situation encountered in molecular systems. By making use of group theoretical arguments, we show that such linear combinations can be written down by simple geometrical considerations through the use of point group character tables, without using extensive numerical computations. Furthermore, we apply this formalism to study the coupling of hierarchical arrays containing a large number of nanoparticles. This theory thus provides an intuitive and formal approach for the rational design of plasmonic nanostructures.

DOI: 10.1103/PhysRevB.81.075414 PACS number(s): 78.67.Bf, 73.20.Mf, 78.20.Bh

I. INTRODUCTION

A great effort is currently being devoted to understanding the optical properties of nanoscale systems, in particular those consisting of metallic nanoparticles (MNPs). Partly, the motivation arises from the fact that the interaction of an electromagnetic (EM) field with MNPs leads to the excitation of surface-plasmon polaritons (SPs): coherent charge oscillations that can occur at metal-dielectric interfaces, which are typically confined to length scales much smaller than the optical diffraction limit. This characteristic has important consequences, for it can lead to strong localization and thus enhancement of electromagnetic fields, a desirable feature in applications such as chemical sensing[1] and radiative-decay control.[2,3]

Several factors influence the optical response of MNPs; these include: composition, surrounding dielectric media, and particle size as well as shape—effects that have been extensively studied in the literature.[4–6] In addition to these parameters, interparticle interaction is also known to play an important role in the optical properties. Two types of interactions can be distinguished, depending on the magnitude of the interparticle separations: (i) near field coupling, relevant for nearly touching particles, and (ii) far-field coupling, which is mediated by the fields scattered by the nanostructures, which are dipolar in nature for particle sizes much smaller than the wavelength. Interesting phenomena arises from these interactions, for they can lead to the formation of super-radiant (bright) and subradiant (dark) modes of the interacting ensemble, which originate when the dipolar modes of each member of the structure oscillate in phase and out of phase, respectively. Furthermore, the interaction of bright and dark modes has been shown to result in narrow Fano[7] resonances,[8–12] and in a plasmonic equivalent of electromagnetically induced transparency,[13,14] both of which have important implications in sensing applications.

Experimentally, interparticle interactions can be easily identified because they result in changes to the scattering spectra. Demonstrated in a recent study,[15] it was found that these spectral changes were also sensitive to the relative orientation between the particles, providing evidence that the coupling of the surface plasmon modes depends on the symmetry of the geometrical arrangement of the MNPs comprising the interacting system. The aim of this paper is to describe these symmetry effects theoretically, by considering the interparticle interactions of symmetric arrangements of subwavelength scale nanoparticles. The theoretical framework for this work is based on the electrostatic approximation, developed by Mayergoyz *et al.*[16] and further extended by Davis *et al.*,[17] but in addition, we present in this paper the connection of this formalism to that of group theory.

The outline of this paper is as follows. In Sec. II we summarize the electrostatic theory of SP resonances in metallic nanoparticles. This involves solutions of an integral equation for the resonant modes of a nanoparticle. The theory is extended to multiple interacting nanoparticles leading to an eigenvalue problem for the coupled system. We show how group theory can be used to construct simple solutions for the SP modes of the system of nanoparticles by exploiting the symmetries in the system. This is followed in Sec. III where we show how the theory works for coupled systems of identical nanorods forming trimers and hexamers. It is shown how this method can be extended to hierarchies of nanoparticle systems. In Sec. IV we provide some examples of where this theory has application, particularly in the design of systems exhibiting dark modes.

II. THEORY

A. Electrostatic resonances in subwavelength scale nanoparticles: Coupling in *N*-particle systems

For a single MNP defined by a surface boundary S, within the quasistatic approximation, the surface charge distribution $\sigma_\alpha^j(\vec{\mathbf{r}})$ of its jth SP mode satisfies the following boundary-integral eigenvalue equation:[16]

$$\sigma_\alpha^j(\vec{\mathbf{r}}) = \frac{\gamma_\alpha^j}{2\pi}\oint \sigma_\alpha^j(\vec{\mathbf{r}}_q)\frac{(\vec{\mathbf{r}}-\vec{\mathbf{r}}_q)}{|r-r_q|^3}\cdot \hat{n}dS_q, \tag{1}$$

where $\hat{n}$ is the normal to the surface of the particle at $\vec{\mathbf{r}}$, and the eigenvalue γ_α^j (a dimensionless quantity) fixes the resonance frequency ω_j. These two quantities are related to the electric permittivity ϵ of the particle by the following relationship:[16]

$$\text{Re } \epsilon(\omega_j) = \epsilon_b\left(\frac{1+\gamma_\alpha^j}{1-\gamma_\alpha^j}\right), \tag{2}$$

with ϵ_b the (assumed to be real) permittivity of the medium surrounding the particle.

Equation (1) describes surface charge distributions that are self-sustained (and source-free) modes of a particle, where the magnitude of $\sigma(\vec{\mathbf{r}})$ arises from the electric field at $\vec{\mathbf{r}}$ associated with the surface charge distribution existing at other positions $\vec{\mathbf{r}}_q$ along the boundary S that defines the particle.

Similar results can be found for the surface dipole distribution $\tau_\alpha^k(\vec{\mathbf{r}})$, and it has been found that: (i) this distribution satisfies an equation that is the adjoint of Eq. (1) with the same set of eigenvalues γ_α^j and (ii) the sets of these two surface distributions are bi-orthogonal,

$$\oint \tau_\alpha^k(\vec{\mathbf{r}})\sigma_\beta^j(\vec{\mathbf{r}})dS = \delta_{\alpha\beta}\delta^{kj}. \tag{3}$$

For an arbitrary array of N nanoparticles, the surface charge distribution can be written as a superposition of the normal modes of each particle of the ensemble

$$\sigma(\vec{\mathbf{r}}) = \sum_{\alpha=1}^{N}\sum_j a_\alpha^j\sigma_\alpha^j(\vec{\mathbf{r}}), \tag{4}$$

This new distribution must also satisfy Eq. (1),

$$\sigma(\vec{\mathbf{r}}) = \frac{\Lambda}{2\pi}\oint \sigma(\vec{\mathbf{r}}_q)\frac{(\vec{\mathbf{r}}-\vec{\mathbf{r}}_q)}{|r-r_q|^3}\cdot \hat{n}dS_q, \tag{5}$$

where in general $\Lambda \neq \gamma$.

The problem that we now wish to solve is that of finding the set of expansion coefficients a_α^j and the new eigenvalues Λ of the system, which result from the electrostatic interaction among the particles.

To proceed, we expand $\sigma(\vec{\mathbf{r}})$ following Eq. (4):

$$\sigma(\vec{\mathbf{r}}) = \sum_{\beta,k} a_\beta^k\sigma_\beta^k(\vec{\mathbf{r}}) = \frac{\Lambda}{2\pi}\sum_{\beta,k}\oint a_\beta^k\sigma_\beta^k(\vec{\mathbf{r}}_\beta)\frac{(\vec{\mathbf{r}}-\vec{\mathbf{r}}_\beta)}{|r-r_\beta|^3}\cdot \hat{n}dS_\beta, \tag{6}$$

We multiply this equation by $\tau_\alpha^m(\vec{\mathbf{r}})$ and integrate over all surfaces, bearing in mind the bi-orthogonality condition of Eq. (3),

$$a_\alpha^m = \frac{\Lambda}{2\pi}\sum_{\beta,k} a_\beta^k\left\{\oint \tau_\alpha^m(\vec{\mathbf{r}})\hat{n}\cdot\oint \sigma_\beta^k(\vec{\mathbf{r}}_\beta)\frac{(\vec{\mathbf{r}}-\vec{\mathbf{r}}_\beta)}{|r-r_\beta|^3}dS_\beta dS\right\}$$

$$= \frac{\Lambda}{2\pi}\sum_{\beta,k} K_{\alpha\beta}^{mk}\cdot a_\beta^k, \tag{7}$$

where we have implicitly defined a coupling coefficient $K_{\alpha\beta}^{mk}$, as the quantity enclosed in brackets in this equation. This equation can be written down using matrix notation as follows:

$$\vec{\mathbf{a}} = \frac{\Lambda}{2\pi}\mathbb{K}\cdot\vec{\mathbf{a}}, \tag{8}$$

and it can be identified as an eigenvalue equation for which the solutions are the roots of the characteristic equation: $\det\{\mathbb{K}-\frac{2\pi}{\Lambda}\mathbb{1}\}=0$, where $\mathbb{1}$ is the $N\times N$ unit matrix. The diagonal elements of $\mathbb{K}$ can be found using the bi-orthogonality condition given by Eq. (3),

$$\delta^{km} = \oint \tau_\alpha^k(\vec{\mathbf{r}})\sigma_\alpha^m(\vec{\mathbf{r}})dS$$

$$= \frac{\gamma_\alpha^k}{2\pi}\oint\oint \tau_\alpha^k(\vec{\mathbf{r}})\sigma_\alpha^m(\vec{\mathbf{r}}_q)\frac{\vec{\mathbf{r}}-\vec{\mathbf{r}}_q}{|r-r_q|^3}\cdot\hat{n}dS_q dS,$$

$$\delta^{km} = \frac{\gamma_\alpha^k}{2\pi}K_{\alpha\alpha}^{km}, \tag{9}$$

where we have substituted for $\sigma_\alpha^m(\vec{\mathbf{r}}_q)$ the expression given by Eq. (1).

With these results, we have thus translated the problem of solving the boundary-integral Eq. (1) for N interacting particles, to an eigenvalue equation [Eq. (8)] that depends on the properties of each member of the ensemble [through the set of γ_α^j and $\sigma_\alpha^j(\vec{\mathbf{r}})$] and the interparticle coupling strength expressed through the off-diagonal elements of the matrix $\mathbb{K}$. More explicitly, for an aggregate of MNPs it is possible to solve the electrostatic problem for each individual particle and then use these solutions to find the optical response of the composite by considering only the interparticle interactions (contained in the matrix $\mathbb{K}$).

For each particle α, solution of Eq. (1) provides the sets γ_α^k and $\sigma_\alpha^k(\vec{\mathbf{r}})$. The values of $K_{\alpha\beta}^{mk}$ depend on the distance between particles α and β as well as on their relative orientation, and physically, it represents the interaction of the surface dipole density of particle α (mth mode) with the electric field produced by the kth SP charge distribution of particle β.

There are other eigenvalue-type approaches that can be used for describing the optical response of collection of nanoparticles, such as the method of Bergmann,[18–23] and the one of Stockmann *et al.*,[24] both of which are written as generalized eigenvalue problems. Noteworthy is the fact that Bergman solved the electromagnetic problem of a collection of spherical objects (pairs or periodic arrays) by first considering each spherical object independently, and later considering the effect of their mutual interaction,[18–22] thus being similar to the method presented by us so far.

B. Symmetry-adapted linear combination of surface charge distributions

If a set of MNPs is spatially arranged forming a geometrical shape that is invariant under a given number of symmetry operations, it is possible to classify this geometrical shape into a point group, which is a collection of symmetry operations R (rotation, reflection, inversion, etc) that, in addition to following particular sets of algebraic rules, transform the geometrical array into an equivalent configuration.

As we have demonstrated in the previous section, the interaction of these particles is described by a coupling matrix $\mathbb{K}$, the elements of which have a dependency on the geometrical distribution of the interacting particles (i.e., separation distance and relative orientations). If the action of any of these symmetry operations R leaves these geometrical factors unchanged, then it would not alter the form of $\mathbb{K}$ and similar to the case encountered in quantum mechanics,[25] it is said that $\mathbb{K}$ and R commute.

Therefore, for any eigenvector $\vec{\mathbf{a}}$ of $\mathbb{K}$ (or physically, any SP mode of the particle array), by virtue of this commutativity, the following relationships hold:

$$\{\mathbb{K}R - R\mathbb{K}\}\vec{\mathbf{a}} = 0,$$

$$\therefore \quad R\mathbb{K}\vec{\mathbf{a}} = \mathbb{K}R\vec{\mathbf{a}} = \frac{2\pi}{\Lambda}R\vec{\mathbf{a}}, \tag{10}$$

which implies that (i) $R\vec{\mathbf{a}}$ is also an eigenvector of the system with the same eigenvalue and also that (ii) R and $\mathbb{K}$ share a common set of eigenvectors.

This last property is very important. This is in part due to the fact that by forming a matrix $\mathbb{S}$ with these eigenvectors $\vec{\mathbf{a}}_S$, it can be shown that[25]

$$\mathbb{S}^T\mathbb{K}\mathbb{S} = \mathrm{diag}\left(\frac{2\pi}{\Lambda}\right), \tag{11}$$

where $\mathrm{diag}(\frac{2\pi}{\Lambda})$ is a diagonal matrix with the eigenvalues of $\mathbb{K}$, which therefore gives the resonance frequency of each SP mode of the interacting system. But more importantly, according to these arguments, the problem of finding the SP modes of a symmetric aggregate of MNPs can be simplified to that of constructing the eigenvectors $\vec{\mathbf{a}}_S$, which are symmetry-adapted linear combinations (SALCs) of the surface charge distributions of each particle in the ensemble. These SALCs are then the new collective eigenmodes of the structures, for which the resonance frequencies are easily found by carrying out a simple matrix multiplication [that of Eq. (11)].

In constructing these SALCs one can then use the machinery of group theory which gives the additional advantage of predicting which of the resulting collective SP modes of a symmetric structure has a net dipole moment or, equivalently, result in a super-radiant SP mode. In the next section, we illustrate the use of this theoretical framework for some particular cases.

III. CASE STUDIES

For definiteness, we consider in this section symmetric aggregates containing subwavelength scale gold nanorods in vacuum (and we use the dielectric data of Johnson and Christy[26]). As stated in the previous section, to find the collective modes of any of such aggregates, it is necessary to know for all the members of the ensemble the eigenvalues of Eq. (1) (equivalently the resonance frequencies) and its eigenmodes (or surface charge distributions). For the sake of simplicity we will consider aggregates containing only one type of such nanorods.

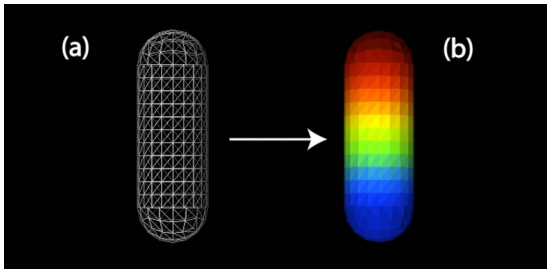

FIG. 1. (Color online) (a) Discretization of the surface S that defines a spherically capped nanorod of 25 units in diameter and 75 units in length (provided that $d \ll \lambda$, these results are scale independent) (b) Plot of the surface charge distribution $\sigma^{(d)}(\vec{\mathbf{r}})$ of the dipolar SP mode, found by numerically solving Eq. (1). For this SP mode, the eigenvalue of Eq. (1) is $\gamma^{(d)} = 1.259$, corresponding to a wavelength of 592 nm. The superscript d denotes the dipolar character of the resonance. The color in the figure gives the relative sign of the charge distribution.

To find the $\sigma_\alpha^k(\vec{\mathbf{r}})$ and γ_α^k for a nanoparticle, the surface S defining this particle is discretized by using a mesh. In Fig. 1(a) we show a triangular mesh constructed along the surface of a nanorod. This discretization of S then allows for a numerical solution of Eq. (1) which, as described in more detail by Mayergoyz *et al.*,[16] consists of solving an eigenvalue problem for a matrix of size $N_t \times N_t$, with N_t the number of triangles used in meshing the surface of the nanorod. The result of such a computation, for the longitudinal dipolar mode of the nanorod, is shown in Fig. 1(b).

In the following, we consider the interaction of only this dipolar resonance in symmetric configurations containing replicas of this nanorod. For these cases, the coupling matrix $\mathbb{K}$ contains equal diagonal elements, with off-diagonal elements involving the same resonance mode,

$$\mathbb{K} = \begin{pmatrix} \frac{2\pi}{\gamma_d} & K_{12} & \cdots & K_{1N} \\ K_{21} & \frac{2\pi}{\gamma_d} & \cdots & K_{2N} \\ \vdots & & \ddots & \vdots \\ K_{N1} & \cdots & & \frac{2\pi}{\gamma_d} \end{pmatrix}. \tag{12}$$

The simplest aggregate of interacting nanoparticles consists of a dimer. However, since such a model system has been extensively studied in the past, we chose to present instead the results for a trimer.

A. Trimers

Let us consider three nanorods arranged on a plane such that the positions of their centroids correspond to the vertices

of an equilateral triangle, thus being invariant with respect to: (i) a rotation of 120 degrees ($2\pi/3$ rad) through the z axis, (ii) 180 degrees rotations through the three axis containing each particle, and (ii) a reflection on the xy plane (a symmetry plane that bisects each particle). These symmetry operations are characteristic of objects belonging to the point group D_{3h}, which in addition to these symmetry operations also contains an improper rotation and three planes of reflections (each one intersecting one particle).[27]

Using the dipolar mode of the nanorods as a basis for a representation Γ of the D_{3h} group, one finds that it has the following irreducible representation $\Gamma = A_1' + E'$, where A_1' (Ref. 40) is a one-dimensional representation of D_{3h}, symmetric with respect to a rotation of 120° on the z axis (in a Cartesian coordinate system, A_1' could be represented by the z axis) and E' is a two-dimensional representation of this group that is antisymmetric with respect to a 180° rotation perpendicular to the plane containing the nanorods (again, in a Cartesian coordinate system, the symmetry operations belonging to E' could be constructed with square matrices of dimension 2, whose operation modify the x and y coordinates). That is, any matrix representing either a symmetry operation on the coordinates of the trimer, or the $\mathbb{K}$ matrix, can be reduced to a combination of a matrix of dimension 2 with a one-dimensional matrix (scalar). By inspection of the dimensionality of such an irreducible expansion, it is obvious that the electrostatic coupling of these particles would lead to three surface charge distributions, two of which (those belonging to E') are degenerate in frequency (energy); additionally, only these two modes are going to have a net dipole moment different from zero (thus being optically active), as we shall discuss later on.

Given the symmetry of the system, and considering only the dipolelike mode of the nanorods of Fig. 1, the coupling coefficients of Eq. (12) are all equal, which therefore fixes the form of the matrix $\mathbb{K}$,

$$\mathbb{K} = \begin{pmatrix} \frac{2\pi}{\gamma_d} & K & K \\ K & \frac{2\pi}{\gamma_d} & K \\ K & K & \frac{2\pi}{\gamma_d} \end{pmatrix}. \tag{13}$$

To obtain the symmetry-adapted combinations of surface charge distributions, we note that these must be symmetric with respect to rotations about the z axis of Fig. 2. This simplifies much of the problem since one could look for linear combinations that are invariant with respect to the purely rotational point group C_3, which only contains three symmetry operations, namely the identity ($\hat{E}$), a rotation of 120° (through the z axis of Fig. 2) denoted by $\hat{C}_3$, and a two–fold rotation by 120° denoted by the symbol $\hat{C}_3^2$.

By inspection of the character table for the C_3 group (given in the Appendix, Table I), a basis for the one-dimensional representation A_1' is given by

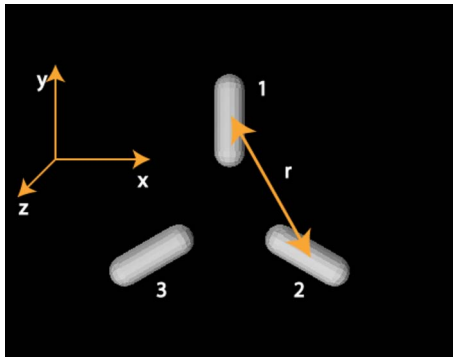

FIG. 2. (Color online) Spatial configuration of nanorods. The centroids of the nanorods are equally spaced by a distance $r = 125$ nm. Each nanorod points to the center of the triangle. The symmetry of this arrangement corresponds to the point group D_{3h} and has an irreducible representation given by $A_1' + E'$.[27] Each nanorod is arbitrarily labeled for the construction of the coupling matrix of the system.

$$\sigma_N^{A_1'}(\vec{\mathbf{r}}) = \frac{1}{\sqrt{3}}(1 \quad 1 \quad 1) \cdot \begin{pmatrix} \sigma_1(\vec{\mathbf{r}}) \\ \sigma_2(\vec{\mathbf{r}}) \\ \sigma_3(\vec{\mathbf{r}}) \end{pmatrix}, \tag{14}$$

which is a normalized function, symmetric with respect to all the symmetry operations of the C_3 group (all the characters for this representation are equal to one).

To find a basis for the E representation we make use of the projection operator[25,27] $\hat{P}^E$,

$$\hat{P}^E \propto \sum_r \chi(r)^E \hat{r}, \tag{15}$$

where $\hat{r}$ is a symmetry operation of the point group and $\chi(r)^E$ is the character of that operation on the E representation (given in Table I).

Application of this operator to the (dipole) surface distribution of the nanorod labeled as 1 in Fig. 2 gives

$$\hat{P}^{E(1)}\sigma_1 \approx \hat{E} \cdot \sigma_1 + \varepsilon \hat{C}_3 \cdot \sigma_1 + \varepsilon^* \hat{C}_3^2 \cdot \sigma_1 = \sigma_1 + \varepsilon\sigma_3 + \varepsilon^*\sigma_2,$$

$$\hat{P}^{E(2)}\sigma_1 \approx \hat{E} \cdot \sigma_1 + \varepsilon^* \hat{C}_3 \cdot \sigma_1 + \varepsilon \hat{C}_3^2 \cdot \sigma_1 = \sigma_1 + \varepsilon^*\sigma_3 + \varepsilon\sigma_2, \tag{16}$$

where $\varepsilon = \exp(2\pi i/3)$, and the asterisk indicates complex conjugation.

One can obtain linear combinations with real coefficients by adding and subtracting the two functions obtained, arriving to the following results:

$$\sigma_N^{E_{(1)}'}(\vec{\mathbf{r}}) = \frac{1}{\sqrt{6}}(2 \quad -1 \quad -1) \cdot \begin{pmatrix} \sigma_1(\vec{\mathbf{r}}) \\ \sigma_2(\vec{\mathbf{r}}) \\ \sigma_3(\vec{\mathbf{r}}) \end{pmatrix}, \tag{17}$$

and

$$\sigma_N^{E_{(2)}'}(\vec{\mathbf{r}}) = \frac{1}{\sqrt{2}}(0 \quad -1 \quad 1) \cdot \begin{pmatrix} \sigma_1(\vec{\mathbf{r}}) \\ \sigma_2(\vec{\mathbf{r}}) \\ \sigma_3(\vec{\mathbf{r}}) \end{pmatrix}. \tag{18}$$

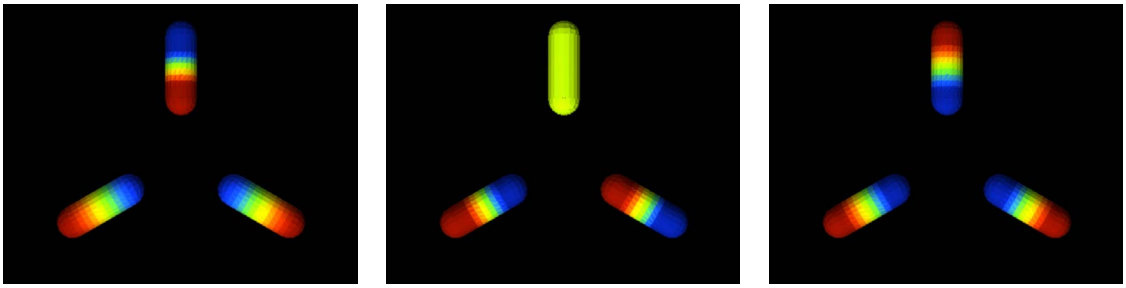

(a) $\sigma_N^{E'_{(1)}} = \frac{1}{\sqrt{6}}(2,-1,-1)$ (b) $\sigma_N^{E'_{(2)}} = \frac{1}{\sqrt{2}}(0,-1,1)$ (c) $\sigma_N^{A'} = \frac{1}{\sqrt{3}}(1,1,1)$

FIG. 3. (Color online) Collective SP modes of the D_{3h}-symmetric configuration of nanorods. The mode corresponding to the A' representation is a dark mode of the structure. Note that for the plotted $\sigma_N^{E'_{(1)}}$ function corresponds to $-1\times$ the one defined in Eq. (17).

With this basis set, we can construct a representation of $\mathbb{S}$ [Eq. (11)], which in the present case reads as follows:

$$\mathbb{S} = \begin{pmatrix} \frac{1}{\sqrt{3}} & \sqrt{\frac{2}{3}} & 0 \\ \frac{1}{\sqrt{3}} & -\frac{1}{\sqrt{6}} & -\frac{1}{\sqrt{2}} \\ \frac{1}{\sqrt{3}} & -\frac{1}{\sqrt{6}} & \frac{1}{\sqrt{2}} \end{pmatrix}. \tag{19}$$

After some simple algebraic manipulation, it can be shown that application of Eq. (11) for the case under consideration produces a diagonal matrix

$$\mathbb{S}^T\mathbb{K}\mathbb{S} = \begin{pmatrix} \frac{2\pi}{\gamma_d} + 2K & 0 & 0 \\ 0 & \frac{2\pi}{\gamma_d} - K & 0 \\ 0 & 0 & \frac{2\pi}{\gamma_d} - K \end{pmatrix} = \frac{2\pi}{\Lambda}. \tag{20}$$

Thus knowledge of γ_d and K will then give the new eigenvalues Λ, or equivalently, the resonance frequencies of the structure of Fig. 2. Direct numerical evaluation of the coupling coefficient K for this structure gives $K=0.027$ and leads therefore to the following set of collective eigenvalues for the structure: $\Lambda=1.251, 1.251, 1.273$, which correspond to wavelengths of 595 ($2\times$ degenerate) and 586 nm.

In Fig. 3, we plot the surface charge distributions for the D_{3h} system as obtained from a numerical solution of Eq. (5). It can be seen that the modes thus obtained correspond to those predicted by simple group theoretical arguments.

In the D_{3h} point group, the dipole moment (a vector) belongs to the irreducible representation[28] $\Gamma_d = E' + A_2''$, which can also be verified by inspection of the character table for this point group (see Table II in the Appendix). As we have analytically derived, only two of the collective SP modes of the system of Fig. 2 transform like the E' representation, for which x and y in a rectangular coordinate system are also a basis set. Therefore only these two modes have a net dipole moment, an assertion that can be checked by the results of Fig. 3. On the contrary, the nondegenerate $\sigma_N^{A'_1}$ distribution has no net dipole moment, this being a direct consequence of the symmetry properties of the A'_1 representation of the D_{3h} point group, and is therefore a subradiant or "dark mode" of the structure. These results could have also been guessed by inspection of the character table of the point group, given the irreducible representation obtained for the dipoles in Fig. 2.

B. Hexamers

In the preceding example, the dimension of the coupling matrix $\mathbb{K}$ allows for direct and simple calculation of its eigenvalues and eigenvectors (it only requires the solution of a polynomial equation of order 3). For structures containing more MNPs, the size of the coupling matrix is expected to increase, apparently precluding a direct (algebraic) solution of the eigenvalue problem of Eq. (8). However, for symmetric structures, it is possible to invoke symmetry to simplify the problem and in this section we illustrate this process for an aggregate containing six MNPs, disposed in the shape of a hexagon, a situation depicted in Fig. 4.

This geometrical arrangement is symmetric with respect to a rotation of $2\pi/6$ (axis of rotation perpendicular to the plane containing the rods), and also to rotations of 180 degrees in the plane (xy) containing the MNPs; furthermore, it is also symmetric with respect to a horizontal reflection (in xy bisecting each rod), thus allowing us to classify this geometric shape as belonging to the point group D_{6h}. This group contains 24 symmetry operations and has 12 irreducible representations.

If we again make use of the dipole mode of each MNP as a basis set, it is straightforward to demonstrate that with this set one can build the following irreducible representation of the point group: $A_{1g}+E_{2g}+B_{1u}+E_{1u}$.[27] This consists of two one-dimensional representations, A_{1g} (symmetric with respect to a $2\pi/6$ rotation on the z axis) and B_{1u} (antisymmetric with respect to a $2\pi/6$ rotation on the z axis) and two two-dimensional ones E_{2g} (symmetric with respect to inversion through the center of the hexagon) and E_{1u} (antisymmetric with respect to inversion through the center of the hexagon). Inspection of the character table for the D_{6h} group indicates that out of this irreducible representation, only E_{1u}, is expected to have a net dipole moment, thus implying that the other four representations, or collective modes, are dark modes of the structure. These assertions are also consistent

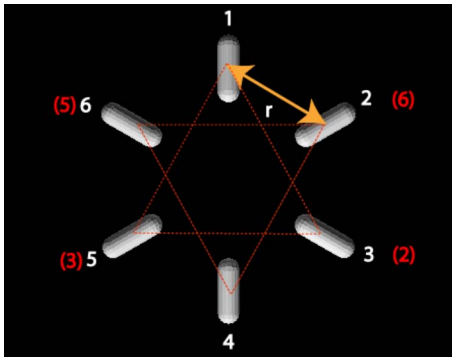

FIG. 4. (Color online) A hexagon of nanorods. The centroids of the nanorods are equally spaced by a distance $r=125$ nm, the coordinate axes are the same as those shown in Fig. 2. Each nanorod points to the center of the hexagon. The symmetry of this arrangement corresponds to the point group D_{6h} and has an irreducible representation given by $A_{1g}+E_{2g}+B_{1u}+E_{1u}$.[27] This system can be thought of as consisting of two interacting trimers (triangles) as indicated with the red dashed lines.

with the fact that in D_{6h}, the dipole moment is represented by a combination involving only A_{2u} (z direction) and E_{1u} (xy directions).[28]

By virtue of the symmetry of the hexagonal arrangement of MNPs, the coupling matrix for this configuration can be written in the following block form:

$$\mathbb{K} = \begin{pmatrix} \mathbb{K}_3 & \mathbb{K}_{ij} \\ \mathbb{K}_{ij}^T & \mathbb{K}_3 \end{pmatrix}, \tag{21}$$

where $\mathbb{K}_3$ describes the interaction of the rods labeled 1, 2, and 3 in Fig. 4,

$$\mathbb{K}_3 = \begin{pmatrix} \frac{2\pi}{\gamma_d} & K_{12} & K_{13} \\ K_{12} & \frac{2\pi}{\gamma_d} & K_{12} \\ K_{13} & K_{12} & \frac{2\pi}{\gamma_d} \end{pmatrix}, \tag{22}$$

where the constants K_{12} and K_{13} have their usual meaning.

The off-diagonal blocks of Eq. (21) describe the coupling between the set of particles {1,2,3} to that of {4,5,6}, which by virtue of the rotational symmetry of the hexagon of Fig. 4 is equivalent to the coupling that exists between the sets {2,3,4} and {5,6,1}, etc. Using similar symmetry arguments, this off-diagonal matrix can be written as follows:

$$\mathbb{K}_{ij} = \begin{pmatrix} K_{14} & K_{13} & K_{12} \\ K_{13} & K_{14} & K_{13} \\ K_{12} & K_{13} & K_{14} \end{pmatrix}, \tag{23}$$

and therefore the problem of describing the interaction of these six particles only requires knowledge of three coupling constants, namely K_{12}, K_{13}, K_{14}.

To find the symmetry-adapted combinations of surface charge distributions for this problem, one would have to apply projection operators for the group D_{6h} in a similar fashion to that done in the case of the trimer. This task is however simplified by noticing that the arrangement of Fig. 4 is also symmetric with respect to the symmetry operations of the point group C_6, which contains only rotations about the z axis (C_6 contains rotations by 60, 120 and 180 degrees). By inspection of the character table of this point group (for reference, it is shown in Table III of the Appendix), the following linear combinations can be constructed:[27]

$$\sigma_A = \frac{1}{\sqrt{6}}(\sigma_1 + \sigma_2 + \sigma_3 + \sigma_4 + \sigma_5 + \sigma_6),$$

$$\sigma_B = \frac{1}{\sqrt{6}}(\sigma_1 - \sigma_2 + \sigma_3 - \sigma_4 + \sigma_5 - \sigma_6),$$

$$\sigma_{E_{1a}} = \frac{1}{\sqrt{12}}(2\sigma_1 + \sigma_2 - \sigma_3 - 2\sigma_4 - \sigma_5 + \sigma_6),$$

$$\sigma_{E_{1b}} = \frac{1}{2}(\sigma_2 + \sigma_3 - \sigma_5 - \sigma_6),$$

$$\sigma_{E_{2a}} = \frac{1}{\sqrt{12}}(2\sigma_1 - \sigma_2 - \sigma_3 + 2\sigma_4 - \sigma_5 - \sigma_6),$$

$$\sigma_{E_{2b}} = \frac{1}{2}(\sigma_2 - \sigma_3 + \sigma_5 - \sigma_6), \tag{24}$$

and it can be shown that these form an orthonormal set.

Use of these functions to apply a similarity transformation, produces a diagonal matrix that contains the following eigenvalues:

$$\frac{2\pi}{\Lambda} = \frac{2\pi}{\gamma_d} + \begin{cases} 2K_{13} + (2K_{12} + K_{14}), \\ 2K_{13} - (2K_{12} + K_{14}), \\ -K_{13} + (K_{12} - K_{14}), & \text{2-fold degenerate} \\ -K_{13} - (K_{12} - K_{14}), & \text{2-fold degenerate.} \end{cases} \tag{25}$$

In Fig. 5 we present the collective surface charge distribution that arise from a full numerical solution of Eq. (1). It can there be noticed the qualitative agreement obtained between the numerical solutions and the symmetry-adapted combinations given in Eq. (24). Additionally, as stated before, only two of these collective modes, namely those of belonging to the two-fold degenerate representation E_{1u}, have a net dipole moment (contained on the xy plane). The other modes are dark modes of this structure and consist of two nondegenerate modes (A_{1g} and B_{1u}) and one two–fold degenerate one (E_{2g}).

Another approach to solve this problem consists of visualizing the system of Fig. 4 as comprised of two interacting triangles, as shown with dashed lines in Fig. 4. For this case, the coupling matrix can be written in the following block form:

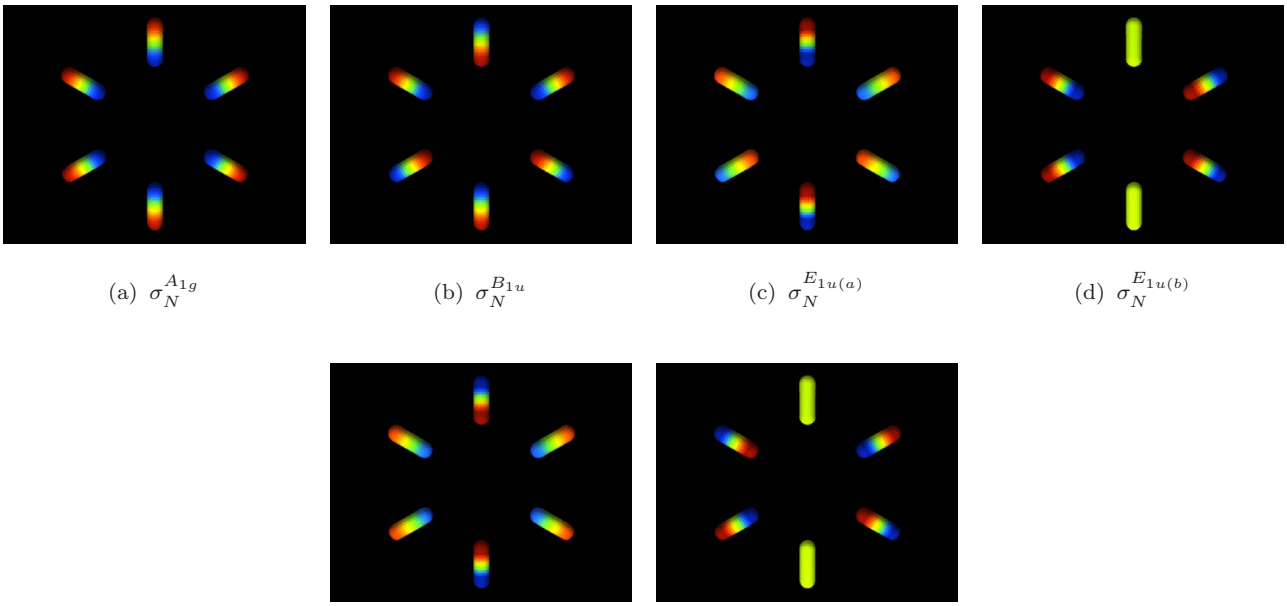

(a) $\sigma_N^{A_{1g}}$ (b) $\sigma_N^{B_{1u}}$ (c) $\sigma_N^{E_{1u(a)}}$ (d) $\sigma_N^{E_{1u(b)}}$

(e) $\sigma_N^{E_{2g(a)}}$ (f) $\sigma_N^{E_{2g(b)}}$

FIG. 5. (Color online) Collective SP modes of the D_{6h}-symmetric configuration of nanorods, labeled according to their symmetry properties. Only those corresponding to the E_{1u} representation are expected to be optically active. These modes were obtained by assuming a distance r=125 nm between adjacent nanorods, which gives the following coupling constants $K_{12}=-1.77\times10^{-2}$, $K_{13}=-5.11\times10^{-3}$, and $K_{14}=-3.83\times10^{-3}$ and eigenvalues (wavelengths): 1.271 (587 nm), 1.251 (595 nm), 1.261 (591 nm), and 1.254 (594 nm).

$$\mathbb{K}=\begin{pmatrix}\mathbb{K}_\Delta & \mathbb{K}_{int}\\ \mathbb{K}_{int}^T & \mathbb{K}_\Delta\end{pmatrix}, \tag{26}$$

where $\mathbb{K}_\Delta$ is the matrix describing the interparticle interaction on each triangle, and is identical (in algebraic form) to that given by Eq. (13). $\mathbb{K}_{int}$ is the matrix that accounts for the coupling that exists between the two triangles, which given the symmetry of the system (and using the labeling in parentheses in Fig. 4) is given by

$$\mathbb{K}_{int}=\begin{pmatrix}K_{14} & K_{15} & K_{15}\\ K_{15} & K_{14} & K_{15}\\ K_{15} & K_{15} & K_{14}\end{pmatrix}. \tag{27}$$

For the symmetric block matrix of Eq. (26), the general eigenvectors are

$$\sigma_N^{(1)}(\vec{\mathbf{r}})=\frac{1}{\sqrt{2}}(1,1)\cdot\begin{pmatrix}\sigma_1(\vec{\mathbf{r}})\\ \sigma_2(\vec{\mathbf{r}})\end{pmatrix}=(\sigma_1(\vec{\mathbf{r}})\oplus\sigma_2(\vec{\mathbf{r}}))/\sqrt{(2)},$$

$$\sigma_N^{(2)}(\vec{\mathbf{r}})=\frac{1}{\sqrt{2}}(1,-1)\cdot\begin{pmatrix}\sigma_1(\vec{\mathbf{r}})\\ \sigma_2(\vec{\mathbf{r}})\end{pmatrix}=(\sigma_1(\vec{\mathbf{r}})\ominus\sigma_2(\vec{\mathbf{r}}))/\sqrt{(2)}, \tag{28}$$

where $\sigma_{1,2}(\vec{\mathbf{r}})$ are the SALCs for each particle trimer, already discussed in the previous section and given by Eqs. (14), (17), and (18).

It can be verified that these functions $\sigma_N^{(1)}(\vec{\mathbf{r}})$ and $\sigma_N^{(2)}(\vec{\mathbf{r}})$ are identical to those found by making use of the full symmetry of the problem, namely, the SALCs given by Eq. (24). The advantage of the approach just presented, resides in the fact that the problem of a six-particle system was simplified to that of two interacting trimers. This suggests that for more complex structures, such as nanoparticle gratings, it is possible to find the collective optical response of the system (not including diffraction and retardation effects) by successively accounting for the interaction of subsets of the particles comprising the structure. In the following section we illustrate this procedure for a particular system.

C. Hierarchical symmetric configurations

So far we have considered the SP resonances for a single nanorod, a trimer of nanorods, and two trimers forming a hexagon. In these two last instances, we have used the symmetry properties of these aggregates to solve the eigenvalue problem of Eq. (8). One could then construct other symmetric configurations by using these aggregates as the building blocks to more complex hierarchical structures, a process that is exemplified in Fig. 6(a).

In the past, it has been demonstrated that large scale, periodic arrays of MNPs can be utilized as surface-enhanced Raman scattering substrates.[29–31] Such arrays typically possess some symmetry properties and are thus amenable to the theoretical techniques that we have employed for the case of the trimer and the hexamer. For illustrative purposes, let us consider the system depicted in Fig. 6(b), which consists of three triangular aggregates of nanorods, where the centroid of each triangle is positioned at the vertex of an equilateral triangle.

For this interacting system, the coupling matrix can be decomposed into the following blocks:

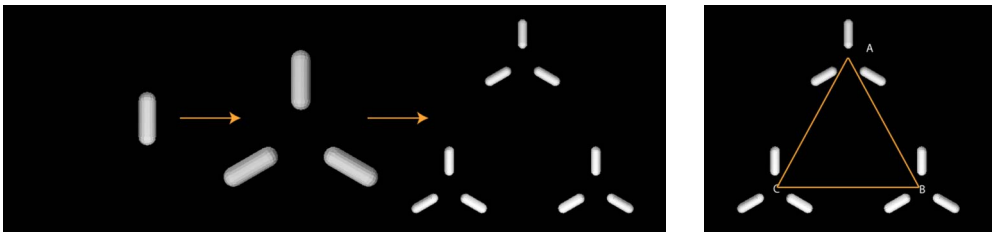

(a) (b)

FIG. 6. (Color online) (a) Construction of hierarchical (symmetric) structures consisting of nanorods. (b) Triangular array of triangular aggregates of nanoparticles. It consists of three trimers positioned in the form of an equilateral triangle. The coordinate axes are the same as those shown in Fig. 2. The symmetry of this arrangement corresponds also to the point group D_{3h}

$$\mathbb{K}_H = \begin{pmatrix} \mathbb{K}_\Delta & \mathbb{K}_{AB} & \mathbb{K}_{AC} \\ \mathbb{K}_{AB}^T & \mathbb{K}_\Delta & \mathbb{K}_{BC} \\ \mathbb{K}_{AC}^T & \mathbb{K}_{BC}^T & \mathbb{K}_\Delta \end{pmatrix}. \tag{29}$$

Here, $\mathbb{K}_\Delta$ is the matrix that describes the interparticle interactions in each triangle (dimension 3×3), and is identical to the one given by Eq. (13). $\mathbb{K}_{AB}$ ($\mathbb{K}_{AC}$) contains all the coupling strength parameters between the triangles in position A with those of B (C), which given the rotational symmetry of the triangle are identical to those describing the interaction between triangles B and C, i.e., $\mathbb{K}_{AB}=\mathbb{K}_{BC}$. Making further use of the rotational symmetry of this arrangement, it can be shown that $\mathbb{K}_{AC}=\mathbb{K}_{AB}^T$, and therefore the coupling matrix $\mathbb{K}_H$ can be simplified to the following generic form:

$$\mathbb{K}_H = \begin{pmatrix} \mathbb{K}_\Delta & \mathbb{K} & \mathbb{K}^T \\ \mathbb{K}^T & \mathbb{K}_\Delta & \mathbb{K} \\ \mathbb{K} & \mathbb{K}^T & \mathbb{K}_\Delta \end{pmatrix}. \tag{30}$$

As we have shown before, in the absence of intertriangle interaction, the collective SP modes of the system are those given by Eqs. (14), (17), and (18). Using the general form of these SALCs to construct a similarity transformation for the matrix (30), it can be shown that it leads to the following block decomposition:

$$\mathbb{V}^T\mathbb{K}_H\mathbb{V} = \begin{pmatrix} \mathbb{K}+\mathbb{K}^T+\mathbb{K}_\Delta & 0 & 0 \\ 0 & -\dfrac{(\mathbb{K}+\mathbb{K}^T-2\mathbb{K}_\Delta)}{2} & \dfrac{\sqrt{3}}{2}(\mathbb{K}-\mathbb{K}^T) \\ 0 & \dfrac{\sqrt{3}}{2}(\mathbb{K}-\mathbb{K}^T) & -\dfrac{(\mathbb{K}+\mathbb{K}^T-\mathbb{K}_\Delta)}{2} \end{pmatrix} = \begin{pmatrix} \mathbb{K}^{A'} & \mathbf{0} \\ \mathbf{0} & \mathbb{K}^{E'} \end{pmatrix}, \tag{31}$$

where the upper block (of dimensions 3×3) originates from the interaction of the A'-symmetric coupling of the normal modes of each triangle. One of such combinations is given by: $(\sigma_A^{E'(1)} \oplus \sigma_B^{E'(1)} \oplus \sigma_C^{E'(1)})/\sqrt{3}$, where the subscript indicates the label of each triangle. Similarly, the lower block (of dimensions 6×6) contains the interaction of E'-symmetric combinations of the modes of each triangle.

Each one of these blocks can be diagonalized separately, and in Fig. 7 we present the results obtained for the $\mathbb{K}^{A'}$ block. All of these modes are also collective dark modes of

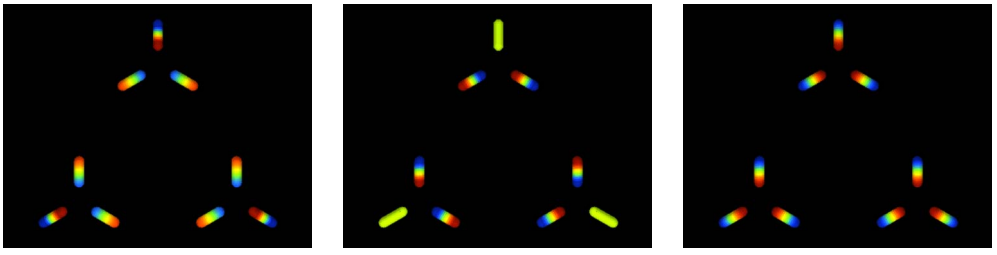

(a) (b) (c)

FIG. 7. (Color online) Collective SP modes of the D_{3h}-symmetric configuration of triangles, obtained by diagonalizing the matrix $\mathbb{K}^{A'}$. It can be noticed that these results are similar to the ones presented in Fig. 3.

the structure, this being a consequence of the symmetry properties of the irreducible representation A'.

IV. DISCUSSION

As we have illustrated, the interaction of symmetric arrays of MNPs can lead to the formation of collective dark SP modes. These modes would not couple directly with plane waves incident on the structures and, likewise, are not expected to be efficient at radiating electromagnetic energy. Hence, it is expected that their excitation (which can be done by a localized emitter[32]) would lead to strong localization of electromagnetic (EM) fields without a background of emitted radiation.[33] These strongly localized EM fields could be beneficial for many applications. For instance, collective dark modes in nanoparticle chains have enabled subwavelength scale waveguiding without radiative losses.[34] Furthermore, it has been found that the highest gain attainable in a "SPASER" (surface plasmon amplification by stimulated emission[35]) is expected to arise from the interaction of a gain medium with the lowest-frequency dark mode of a plasmonic resonator.[33]

In the study of Li *et al.*,[33] these plasmonic resonators consisted of center-symmetric linear arrays of spherical MNPs. The simplest of such arrays consists of a particle dimer. In this case the authors of that work found that the lowest-frequency dark mode for this structure is two-fold degenerate, a feature that has a negative impact on the gain attainable in a SPASER. By increasing the number of particles (among other parameters) they were able to lift this degeneracy and thus obtain nondegenerate dark modes with associated higher gains. It is in this type of situations where the formalism presented in this paper can be extremely useful. This is due to the fact that by simple inspection of point group character tables, it is possible to design symmetric MNP arrays with dark modes of a given degeneracy.

We have shown that by forming an equilateral triangle of nanorods, a nondegenerate dark mode is expected to result from the interaction of the particles [shown in Fig. 3(a)]. Furthermore, for a hexagonal array, we have demonstrated that three dark modes can be supported by the structure, one of which is two-fold degenerate. Likewise, one can conceive other geometrical arrangements and quickly evaluate the number and degeneracy of such dark modes by inspection of respective character tables. The *design* of the frequency of such modes must be carried out numerically; however, the simplicity of the surface-integral eigenvalue problem of Eq. (1) for single particles and the eigenvalue problem for interparticle interactions given by Eq. (8) do not pose, in this regard, a significant limitation.

As we have shown in Sec. III C, the analysis of the SP modes of a large hierarchical structure can be decomposed into that corresponding to smaller substructures of the system. This is extremely advantageous for the reasons just discussed, but additionally it allows a reduction in the scale of the computational problem. However, the applicability of the electrostatic approximation of Eq. (1), is limited to cases when the particle(s) are smaller than the wavelength of an incident electromagnetic field. This implies that for large aggregates, such as the one presented in Sec. III C, additional effects, such as retardation and radiation damping, must be accounted for in the formalism for it to give accurate results.

The formalism presented here is analogous to that employed in molecular orbital theory, where the wave functions describing the molecular orbitals are written as symmetry-adapted linear combinations of atomic orbitals, this in turn being the wave functions of the electrons belonging to molecular constituents (atoms or functional groups).[25,27] In this way the methods discussed in this paper are analogous to the plasmon hybridization model of Nordlander and co-workers.[36–39] At this point it is also worth noting that group theory has been employed within the context of the plasmon hybridization model,[9,38] to classify and interpret some features of the resulting collective SP modes of the interacting systems.

Although we have only considered the interaction of dipolar resonances, the procedure here described is also applicable to higher multipole moments and their interaction, a situation that may arise when the interparticle distances are small.

V. CONCLUSION

Based on the electrostatic approximation,[16] we have derived an equation that relates the collective SP modes of an ensemble of MNPs to those of the individual particles, which simplifies, at least conceptually, the problem of interacting particles. Coupling between the SP modes of particles was found to be dipolelike and is determined by factors such as inter–particle distance and orientation.

For symmetric aggregates of MNPs, the collective SP modes were found to correspond to symmetry-adapted linear combinations of the SP modes of each particle of the aggregate. This situation is analogous to the plasmon hybridization model, and provides an intuitive approach for the design of subwavelength scale optical devices, such as antennas and resonators.

APPENDIX: CHARACTER TABLES FOR THE D_{3h}, C_3 AND C_6 POINT GROUPS

In this appendix, we present the character tables for the point groups C_3, D_{3h}, and C_6. The symbol $\hat{E}$ represents the identity operation, $\hat{C}_n$ rotations of $2\pi/n$, $\hat{\sigma}_h$ and $\hat{\sigma}_v$ planes of reflection, and $\hat{S}_n$ an axis of improper rotation.[25,27] For the point groups C_3 and C_6, the symbols $\hat{C}_n^m$ denote sequential m-fold rotations of $2\pi/n$.

TABLE I. Character table for the C_3 point group, adapted from Ref. 27. Here $\epsilon=\exp(i2\pi/3)$.

C_3	$\hat{E}$	$\hat{C}_3$	$\hat{C}_3^2$	
A	1	1	1	z
E	1	ϵ	ϵ^*	(x,y)
	1	ϵ^*	ϵ	

TABLE II. Character table for the D_{3h} point group, adapted from Ref. 27.

D_{3h}	$\hat{E}$	$2\hat{C}_3$	$3\hat{C}_2$	$\hat{\sigma}_h$	$2\hat{S}_3$	$3\hat{\sigma}_v$	
A_1'	1	1	1	1	1	1	
A_2'	1	1	−1	1	1	−1	
E'	2	−1	0	2	−1	0	(x,y)
A_1''	1	1	1	−1	−1	−1	
A_2''	1	1	−1	−1	−1	1	z
E''	2	−1	0	−2	1	0	

TABLE III. Character table for the C_3 point group, adapted from Ref. 27. Here $\epsilon=\exp(i2\pi/6)$.

C_6	$\hat{E}$	$\hat{C}_6$	$\hat{C}_3$	$\hat{C}_2$	$\hat{C}_3^2$	$\hat{C}_6^5$	
A	1	1	1	1	1	1	z
B	1	−1	1	−1	1	−1	
E_1	1	ϵ	$-\epsilon^*$	−1	$-\epsilon$	ϵ^*	(x,y)
	1	ϵ^*	$-\epsilon$	−1	$-\epsilon^*$	ϵ	
E_2	1	$-\epsilon^*$	$-\epsilon$	1	$-\epsilon^*$	$-\epsilon$	
	1	$-\epsilon$	$-\epsilon^*$	1	$-\epsilon$	$-\epsilon^*$	

The first column of each character table contains the Mulliken symbols that denote the irreducible representations of each group. Briefly, according to this notation, the letters A and B designate one-dimensional representations, whereas E is used for two-dimensional ones. The primes and double primes on these symbols indicate, respectively, that a given representation is symmetric or antisymmetric with respect to a horizontal plane of reflection σ_h, which is also represented by the sign of the character of the representation for this symmetry operation.

According to the last column of Table I, any vector (such as a dipole moment) in a Cartesian coordinate system has an irreducible representation given by $E'+A_2''$ in the D_{3h} point group.

[1] M. Moskovits, Rev. Mod. Phys. **57**, 783 (1985).
[2] D. E. Chang, A. S. Sorensen, P. R. Hemmer and M. D. Lukin, Phys. Rev. Lett. **97**, 053002 (2006).
[3] W. Zhang, A. O. Govorov and G. W. Bryant, Phys. Rev. Lett. **97**, 146804 (2006).
[4] P. Mulvaney, Langmuir **12**, 788 (1996).
[5] K. L. Kelly, E. Coronado, L. L. Zhao, and G. C. Schatz, J. Phys. Chem. B **107**, 668 (2003).
[6] L. M. Liz-Marzán, Langmuir **22**, 32 (2006).
[7] U. Fano, Phys. Rev. **124**, 1866 (1961).
[8] F. Hao, Y. Sonnefraud, P. V. Dorpe, S. A. Maier, N. J. Halas, and P. Nordlander, Nano Lett. **8**, 3983 (2008).
[9] N. A. Mirin, K. Bao, and P. Nordlander, J. Phys. Chem. A **113**, 4028 (2009).
[10] F. Hao, P. Nordlander, Y. Sonnefraud, P. V. Dorpe, and S. A. Maier, ACS Nano **3**, 643 (2009).
[11] T. Pakizeh, C. Langhammer, I. Zoric, P. Apell, and M. Kall, Nano Lett. **9**, 882 (2009).
[12] N. Verellen, Y. Sonnefraud, H. Sobhani, F. Hao, V. V. Moshchalkov, P. V. Dorpe, P. Nordlander, and S. A. Maier, Nano Lett. **9**, 1663 (2009).
[13] S. Zhang, D. A. Genov, Y. Wang, M. Liu and X. Zhang, Phys. Rev. Lett. **101**, 047401 (2008).
[14] N. Liu, L. Langguth, T. Weiss, J. Kastel, M. Fleischhauer, T. Pfau, and H. Giessen, Nat. Mater. **8**, 758 (2009).
[15] A. M. Funston, C. Novo, T. J. Davis, and P. Mulvaney, Nano Lett. **9**, 1651 (2009).
[16] I. D. Mayergoyz, D. R. Fredkin, and Z. Zhang, Phys. Rev. B **72**, 155412 (2005).
[17] T. J. Davis, K. C. Vernon, and D. E. Gómez. Phys. Rev. B **79**, 155423 (2009).
[18] D. J. Bergman, Phys. Rep. **43**, 377 (1978).
[19] D. J. Bergman, J. Phys. C **12**, 4947 (1979).
[20] D. J. Bergman, Phys. Rev. B **19**, 2359 (1979).
[21] D. J. Bergman, Solid State Phys. **46**, 147 (1992).
[22] Y. Kantor and D. J. Bergman, J. Phys. C **15**, 2033 (1982).
[23] D. J. Bergman and D. Stroud, Phys. Rev. B **22**, 3527 (1980).
[24] M. I. Stockman, S. V. Faleev, and D. J. Bergman, Phys. Rev. Lett. **87**, 167401 (2001).
[25] M. Tinkham, *Group Theory and Quantum Mechanics* (McGraw-Hill, New York, 1964).
[26] P. B. Johnson and R. W. Christy, Phys. Rev. B **6**, 4370 (1972).
[27] A. F. Cotton, *Chemical Applications of Group Theory*, 3rd ed. (Wiley, New York, 1990).
[28] A. Gelessus, W. Thiel, and W. Weber, J. Chem. Educ. **72**, 505 (1995).
[29] A. D. McFarland, M. A. Young, J. A. Dieringer, and R. P. Van Duyne, J. Phys. Chem. B **109**, 11279 (2005).
[30] L. Lu, I. Randjelovic, R. Capek, N. Gaponik, J. Yang, H. Zhang, and A. Eychmuller, Chem. Mater. **17**, 5731 (2005).
[31] F. Le, D. W. Brandl, Y. A. Urzhumov, H. Wang, J. Kundu, N. J. Halas, J. Aizpurua, and P. Nordlander, ACS Nano **2**, 707 (2008).
[32] M. Liu, T.-W. Lee, S. K. Gray, P. Guyot-Sionnest and M. Pelton, Phys. Rev. Lett. **102**, 107401 (2009).
[33] K. Li, X. Li, M. I. Stockman, and D. J. Bergman, Phys. Rev. B **71**, 115409 (2005).
[34] S. A. Maier, P. G. Kik, H. A. Atwater, S. Meltzer, E. Harel, B. E. Koel, and A. A. Requicha, Nat. Mater. **2**, 229 (2003).
[35] D. J. Bergman and M. I. Stockman, Phys. Rev. Lett. **90**, 027402 (2003).
[36] E. Prodan, C. Radloff, N. J. Halas, and P. Nordlander, Science **302**, 419 (2003).
[37] E. Prodan and P. Nordlander, J. Chem. Phys. **120**, 5444 (2004).
[38] D. W. Brandl, N. A. Mirin, and P. Nordlander, J. Phys. Chem. B **110**, 12302 (2006).
[39] H. Wang, D. W. Brandl, P. Nordlander, and N. J. Halas, Acc. Chem. Res. **40**, 53 (2007).
[40] We make use of the Mulliken notation for the irreducible representations.